doi:10.3788/gzxb20164505.0516001

Si 衬底上插入 SiO_2 膜对 Ag 纳米颗粒陷光性能的影响

白一鸣,延玲玲,王艳宁,苏琳,刘海,陈诺夫,姚建曦
(华北电力大学 新能源电力系统国家重点实验室,北京 102206)

摘 要:采用磁控溅射法在 Si 衬底上制备了 SiO_2 介质膜,系统地研究了 SiO_2 膜引入对 Ag 纳米颗粒的表面覆盖率、形貌、形成机理和光学性质的影响.研究发现引入 SiO_2 介质膜后,Ag 纳米颗粒的表面覆盖率显著增加,平均粒径明显降低.基于现有的 Ag 纳米颗粒形成机理,提出了粗糙表面 Ag 膜断裂模型以解释其形貌发生变化的原因.紫外-可见光分光光度计测试表明,引入 SiO_2 膜并优化其厚度,可使 Ag 纳米颗粒的偶极消光峰最大红移 86nm,但消光峰强度明显下降.数值模拟计算表明,引入 SiO_2 膜的 Ag 纳米颗粒所能散射的光子数量最小减少 2×10^{18} 个.因此,在 Si 衬底上沉积 SiO_2 膜,不利于 Ag 纳米颗粒陷光性能的提高.

关键词:二氧化硅膜;银纳米颗粒;形成机理;消光谱;陷光性能
中图分类号:O0436.2 **文献标识码**:A **文章编号**:1004-4213(2016)05-0516001-6

Influence of the Silica Films Inserted into Silicon Substrate on the Light Trapping Performance of Silver Nanoparticles

BAI Yi-ming, YAN Ling-ling, WANG Yan-ning, SU Lin, LIU Hai, CHEN Nuo-fu, YAO Jian-xi
(*State Key Laboratory of Alternate Electrical Power System with Renewable Energy Sources, North China Electric Power University*, 102206 *Beijing*, *China*)

Abstract: Introducing silica dielectric film deposited by magnetron sputtering on silicon substrates, the dependence of the surface coverage ratio, morphology, formation mechanism and optical properties for silver nanoparticles on silica dielectric film was exploited. The results indicate that the surface coverage ratios of silver nanoparticles increase but the mean diameters for silver nanoparticles decrease obviously after introducing silica dielectric film. The reason of morphological evolution for silver nanoparticles was explained by an improved model for silver film rupture based on the formation mechanism of silver nanoparticles. A red shift of up to 86 nm of the dipole extinction peak of silver nanoparticles is realized by adjusting the thickness of the silica film but the peak intensity decrease greatly, as analyzed by an ultraviolet-visible spectrophotometer. Numerical simulations of the optimized structures demonstrate that the number of scattered photons by the silver nanoparticles is decreased by as much as 2×10^{18} after inserting a silica layer. Therefore, it is undesirable to deposit silica layer on silicon substrate before silver nanoparticle formation for the light trapping performance of silver nanoparticles.

Key words: Silica film; Ag nanoparticles; Formation mechanism; Extinction spectra; Light trapping performance
OCIS Codes: 160.4236; 160.4760; 290.4020; 290.2200; 290.5850

Foundation item: The National Natural Science Foundation of China (Nos. 61006050, 61076051), the Natural Science Foundation of Bei Jing(No. 2151004), the National High Technology Research and Development Program of China (No. 2011AA50507), the Fundamental Research Funds for the Central Universities (No. 13ZD05).
First author: Bai Yi-ming (1979-), female, associate professor, engineering doctoral degree, mainly focus on new energy materials, nano material science and nanotecenology, Email: ymbai@ncepu.edu.cn.
Received: Oct. 22, 2015; **Accepted**: Jan. 7, 2016

0 Introduction

The fascinating optical and anti-corrosion properties of silica (SiO_2) thin films have attracted great interest in the fields of optics[1-2], microelectronics[3], optoelectronics[4] and sensing[5]. In photovoltaic devices, SiO_2 thin films are often used as an antireflection coating to reduce surface reflection, or as a passivation film to minimize surface recombination [6]. Recently, SiO_2 thin films have been used to modulate the local dielectric environment of plasmonic Nanoparticles (NPs) to enhance the light absorption and performance of thin-film solar cells [7-9]. Beck et al. achieved a 23% increase of optical absorption at 600 nm by introducing a SiO_2 thin film between the silicon substrate and silver (Ag) NPs[10]. Similarly, Xu et al. realized relative enhancements of 41.7% in the short-circuit current density and 41.9% in the efficiency of silicon solar cells by inserting a 35-nm-thick SiO_2 layer [11]. Xu et al. reported that a distinct decrease in reflection can be obtained through the surface plasmonic effect of Ag NPs and antireflective behavior of a SiO_2 layer [12]. The advantages of introducing a SiO_2 layer into light-trapping structures based on plasmonic NPs have been identified [13-16]. However, further studies are still imperative to better understand the effect of a SiO_2 layer on the optical properties of Ag NPs. Moreover, the effects of a high Surface Coverage Ratio (SCR) and Ag particles with an extremely wide size distribution after introducing a SiO_2 layer on the properties of Ag NPs have not yet been examined. In this study, the effect of introducing a SiO_2 film onto Si substrates on the morphology, rupture mechanism and light-trapping behavior of Ag NPs is investigated.

The morphology of Ag NPs on Si wafers before and after the insertion of SiO_2 film are evaluated. The SCR of Ag NPs increases markedly after inserting a SiO_2 film, and decreases as the SiO_2 film thickness increases. To explain the observed increase of SCR and wide size distribution of Ag NPs, a new physical interpretation of the rupture mechanism of the stained Ag film on substrates with different surface roughness is speculated. After introducing a SiO_2 film, the dipole extinction peaks of the Ag NPs exhibit a red shift, broaden, and decrease in intensity. Overall, the number of absorbed photons by the Ag NPs was similar for structures with and without a SiO_2 film.

1 Experimental

SiO_2 thin films of different thickness were fabricated on p-type Si (100) substrates by Radio-Frequency (RF) magnetron sputtering (Huiyu, JB-650). The deposition rate was about 42 nm/min when the RF power was 80 W. The working pressure and substrate temperature were kept at 0.7 Pa and room temperature, respectively. Considering that SiO_2 thin films play the roles of both antireflection and passivation, the desired thickness of a SiO_2 film should range from 40 to 100 nm. Therefore, deposition times of 60, 90 and 120 s were used.

Ag films with a thickness of 7.5 nm were then deposited on the SiO_2 thin films and a bare Si wafer by magnetron sputtering (Huiyu, MS-JB550A) using a sputtering power of 20 W and working pressure of 0.5 Pa at room temperature. The samples were annealed at 500℃ for 1 h under N_2 atmosphere by rapid thermal annealing with a heating rate of 100℃/s. The SiO_2 samples are labeled Ag-SiO_2-60, Ag-SiO_2-90 and Ag-SiO_2-120, according to their SiO_2 deposition time, and the control sample is named Ag-Si. A schematic diagram of the studied structure is depicted in Fig. 1.

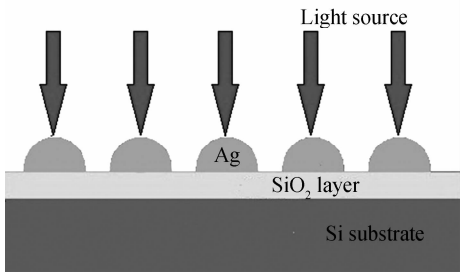

Fig. 1 Schematic diagram of the experimental and theoretical structure

The surface morphologies of the samples were analyzed by Scanning Electron Microscopy (SEM; Quanta 200F). The optical properties of the films were measured by an ultraviolet-visible spectrophotometer (Cary 5000). X-ray Diffraction (XRD) measurements were obtained in a θ-2θ scan mode using a diffractometer (Panalytical X'Pert-MPD Pro) with a Cu $K\alpha$ X-ray source. Image-J software was used to calculate the SCR and Mean Diameter (MD) of Ag NPs.

2 Results and discussion

Fig. 2 shows a typical cross-sectional SEM image of a SiO_2 film formed with a deposition time of 30 s. The SiO_2 film is about 21.8 nm thick. With the same deposition rate, the thicknesses of SiO_2 films formed with deposition times of 60, 90 and 120 s are about 43.6, 65.4 and 87.21 nm, respectively.

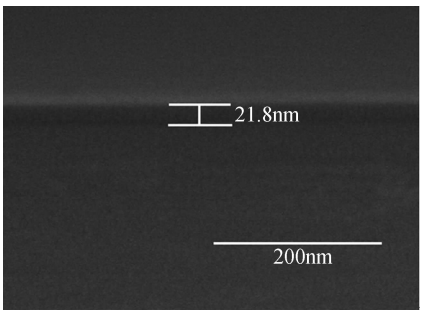

Fig. 2 Typical cross-sectional SEM image of a SiO_2 film formed after 30 s of deposition

An XRD pattern for a SiO_2 film formed with a deposition time of 120 s is presented in Fig. 3, and the inset shows an XRD pattern for the same sample measured with a lower intensity. The weak peak at around 63.61° is consistent with (422) reflection of a SiO_2 film, which suggests that the SiO_2 film has an amorphous-microcrystalline structure. The intensity of the peak is very weak, because the SiO_2 film is thin in comparison with the Si substrate.

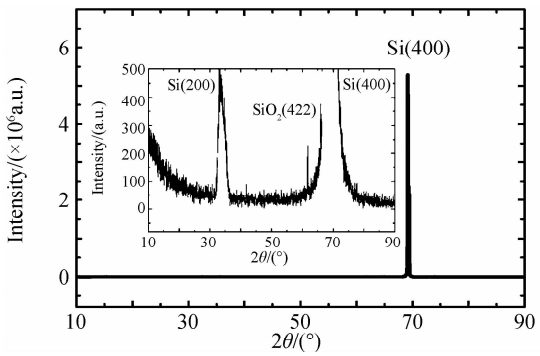

Fig. 3 XRD pattern of a SiO_2 film formed with a deposition time of 120 s. The inset shows a pattern for the same sample measured at lower intensity

Plane-view SEM images of Ag-Si, Ag-SiO_2-60, Ag-SiO_2-90 and Ag-SiO_2-120 are presented in Fig. 4. The SCR of the Ag NPs increased markedly and MD decreased after introducing a SiO_2 layer. The edges of the Ag NPs are not smooth compared with those on the bare Si substrate. The SCRs are 34.1%, 33.5% and 33.2% for Ag-SiO_2-60, Ag-SiO_2-90 and Ag-SiO_2-120, respectively, and are higher than that of the Ag NPs on a bare Si substrate. MD generally decreases as SCR increases. The Ag NPs possess an extremely wide size distribution after introducing a SiO_2 layer, with MD of 59.20, 59.95 and 68.98 nm for Ag-SiO_2-60, Ag-SiO_2-90 and Ag-SiO_2-120, respectively. In contrast, the SCR and MD of Ag NPs on a bare Si substrate are 24.7% and 78.2 nm, respectively. The SCR and MD values are plotted against SiO_2 deposition time in Fig. 5. We speculate that the changes of SCR and MD of the Ag NPs were mainly caused by the surface roughness of SiO_2.

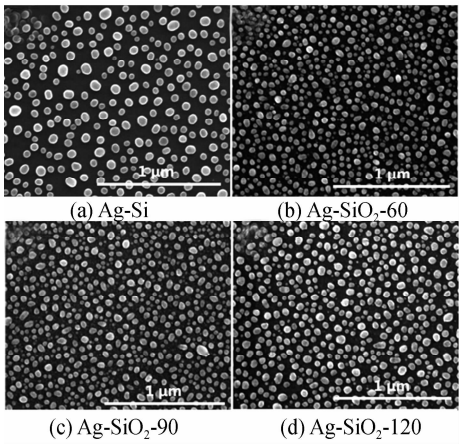

Fig. 4 Plane-view SEM images of samples

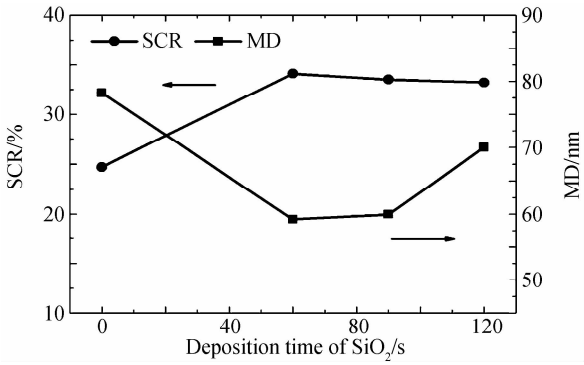

Fig. 5 Dependence of SCR and MD of Ag NPs on the deposition time of SiO_2 films

To fully appreciate the distinct morphology of Ag NPs after inserting different thickness SiO_2 layers on Si substrates, the rupture mechanism of the Ag film to form NPs was investigated by modifying an existing model, which is shown in Fig. 6. Fig. 6(a) illustrates a strained film with a thickness of D prepared on the smooth surface of a semi-infinite substrate. D was uniform before annealing, but then the film was perturbed to form a wavy shape during annealing because of hydrodynamic dewetting instability. The perturbed film thickness z can be given as[17]

$$z = D + q\cos\frac{2\pi x}{\lambda} \tag{1}$$

where q is the wave amplitude, λ is the wavelength and the x axis coincides with the film - substrate interface. The fluctuation in film thickness can be amplified as long as it can absorb adequate energy, and this causes the film to rupture. Film rupture first occurs when

$$\frac{dz}{dx} = 0 \tag{2}$$

We can determine a series of x by solving the periodic Eqs. (1) and (2). The length between two maximum x or two minimum x is defined as the characteristic length Δx, namely, the periodic length. The ruptured film forms a polygon network of connected strings containing a given number of random

holes. Last, the strings break up, shrink and eventually coalesce into NPs [18]. Δx for Ag-Si is 162.8 nm according to the statistical results determined using Image-J software.

However, this model is not suitable for a strained film fabricated on a substrate with an uneven surface, so the model needs to be modified. The perturbed film thickness during heat treatment can be expressed as

$$z=D+q\cos\frac{2\pi x}{\lambda}+H(x) \tag{3}$$

where, $H(x)$ is a function of film surface roughness of the SiO_2 layer. Therefore, Δx can be determined easily using Eqs. (2) and (3) if the function $H(x)$ can be calculated. The fluctuation of the thickness of the Ag film occurs and amplifies during the annealing process, and the Ag film ruptures at points where there is both a valley in the perturbed Ag film and raised point in the SiO_2 layer. A larger number of random holes are generated at these points (compared with the bare Si layer) because of the uneven surface of the SiO_2 layer. Finally, the ruptured films shrink and coalesce into NPs provided there is adequate energy [18]. The edges of the Ag NPs are jagged, and the number of Ag NPs is increased because of the uneven surface of the SiO_2 layer. Therefore, the influence of surface roughness of the SiO_2 layer on the perturbed Ag film maybe the main reason for the obvious changes of shape and SCR of the Ag NPs. Δx for Ag-SiO_2-60, Ag-SiO_2-90 and Ag-SiO_2-120 are 89.6, 90.7 and 90.6 nm, respectively. Moreover, the argon flow may have altered the surface roughness of the SiO_2 films as reported previously[19], this warrants further study.

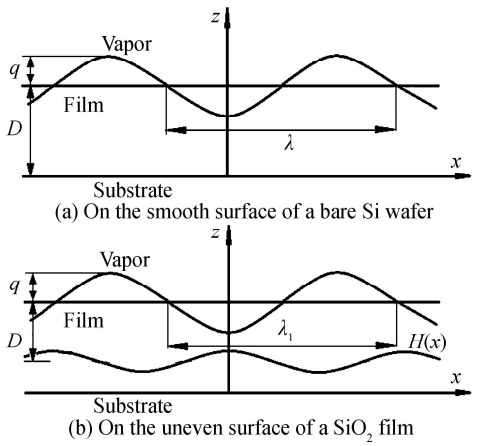

Fig. 6 Schematic diagrams of a perturbed film on different substrates

To investigate the effect of the thickness of the SiO_2 layer on the optical properties of Ag NPs, extinction spectra of the samples were measured. The spectra are displayed in Fig. 7. The position of the dipole extinction peak exhibits an obvious red shift as the deposition time of the Ag films increases. The red shift of the peaks can be attributed to changes of dielectric environment as the SiO_2 gets thicker [11, 14]. The Full Width at Half Maximum (FWHM) also increases with deposition time, indicating that the peaks are broadened. However, the intensity of the peaks decreases after introducing a SiO_2 film. The wider size distribution of the Ag NPs formed on thicker SiO_2 layers leads to the increase of FWHM and decrease of intensity [20-23]. The increase of SCR also contributes to the increase of FWHM, because it causes stronger dipole-dipole interactions. The decrease in size of the Ag NPs formed on thicker SiO_2 layers is another reason for the decrease of peak intensity [24].

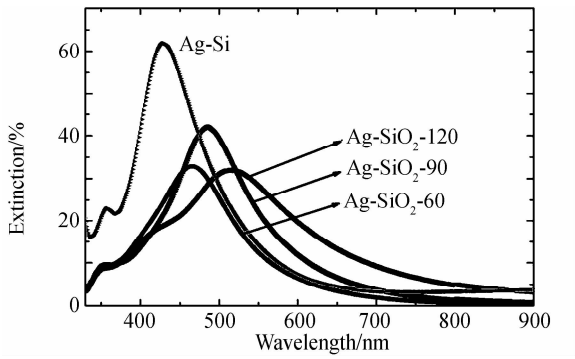

Fig. 7 Experimental extinction spectra for Ag-Si, Ag-SiO_2-60, Ag-SiO_2-90 and Ag-SiO_2-120

The red shift of the peaks and large FWHM obtained after the insertion of a SiO_2 layer should improve the light-trapping performance of metallic NPs, but the lower extinction efficiency is adverse for harvesting photons. Consequently, it is necessary to calculate the number of scattered photons for the samples. The number of scattered photons N_p of the Ag NPs on a bare Si wafer and SiO_2 layer without considering the quantum efficiency of the solar cell can be written as

$$N_p=\int_{\lambda_1}^{\lambda_2}\Phi_0(\lambda)\eta_{ext}(\lambda)\eta_{sca}\,d\lambda \tag{4}$$

where $\Phi_0(\lambda)$ is the standard AM1.5 photon flux, $\eta_{ext}(\lambda)$ is the experimental extinction efficiency of Ag NPs, and λ_1 and λ_2 are 300 and 1000 nm, respectively. η_{sca} is the theoretical scattering ratio because the extinction of NPs is composed of scattering and absorption according to Mie theory, which can be expressed as

$$\eta_{sca}=Q_{sca}/Q_{ext} \tag{5}$$

where Q_{ext} and Q_{sca} are the cross sections of extinction and scattering, respectively, which are given by

$$Q_{ext}=2\pi/k^2\sum_{n=1}^{\infty}(2n+1)\mathrm{Re}(a_n+b_n) \tag{6}$$

$$Q_{sca}=2\pi/k^2\sum_{n=1}^{\infty}(2n+1)(|a_n|^2+|b_n|^2) \tag{7}$$

Here, a_n and b_n are the scattering coefficients of the scattering electromagnetic mode, $k=2\pi N/\lambda$, N is the refractive index of the medium, and λ is the wavelength[25].

The numbers of scattered photons determined for Ag-SiO_2-60, Ag-SiO_2-90, Ag-SiO_2-120 and Ag-Si from numerical simulations are 9.42×10^{19}, 1.39×10^{20} and 2.01×10^{20} and 2.03×10^{20}, respectively. Although the number of scattered photons increases with the thickness of the SiO_2 film, it is decreased by the incorporation of a SiO_2 film compared with that of Ag NPs formed on bare Si. The reductive number of scattered photons at least by the Ag NPs is 2×10^{18} after inserting a SiO_2 layer. Furthermore, numerous small NPs are formed after the incorporation of SiO_2, which will weaken their light scattering effect. Therefore, it is reasonable to conclude that it is not productive to introduce a dielectric film because its rough surface is not favorable to obtain NPs with desirable light-scattering properties. The influence of process parameters on the surface roughness of the SiO_2 layer should be studied to determine if smooth SiO_2 films can be fabricated.

3 Conclusions

The SCR and MD of Ag NPs changed markedly after introduction of a SiO_2 film on a Si substrate. Theoretical analysis of the characteristic length of the Ag NPs formed on the SiO_2 films confirmed that the main reason for the morphological change of the Ag NPs was the rough surface of the SiO_2 layer. The dipole extinction peak of the Ag NPs showed an obvious red shift, FWHM increased, and extinction efficiency decreased after introducing a SiO_2 film. Based on the calculated number of scattered photons by the Ag NPs, it can be concluded that it is unnecessary to introduce a SiO_2 layer, we speculate that its rough surface changes the morphology of the Ag NPs, which weakens their light-trapping ability.

Reference

[1] LIN Ting, ZHANG Yong-ai, CHU Zi-hang, *et al*. Study of controllable full resolution liquid crystal grating based on time division[J]. *Acta Photonica Sinica*, 2015, **44**(11): 1105003

[2] ZHANG Wen-tao, ZHU Bao-hua, WANG Jie-jun. Simulation of transmission characteristics for multilayer film[J]. *Acta Photonica Sinica*, 2014, **43**(Sup. 1): 0131001

[3] LIU Zheng-qi, YU Mei-dong, HUANG Shan, *et al*. Enhancing refractive index sensing capability with hybrid plasmonic - photonic absorbers[J]. *Journal of Materials Chemistry C*, 2015, **3**(17): 4222-4226.

[4] LIU Jun, Wu Gen-Zhu, CHEN Da-ru, *et al*. Metallo-dielectric confined semiconductor microdisk lasers[J]. *Acta Photonica Sinica*, 2012, **41**(12): 1464-1469

[5] LIU Gui-qiang, YU Mei-dong, LIU Zheng-qi, *et al*. One-process fabrication of metal hierarchical nanostructures with rich nanogaps for highly-sensitive surface-enhanced Raman scattering[J]. *Nanotechnology*, 2015, **26**(18): 185702.

[6] OH S J, CHHAJED S, POXSON D J, *et al*. Enhanced broadband and omni-directional performance of polycrystalline Si solar cells by using discrete multilayer antireflection coatings [J]. *Optics Express*, 2013, **21**(1): A157-A166.

[7] PILLAI S, BECK F J, CATCHPOLE K R, *et al*. The effect of dielectric spacer thickness on surface plasmon enhanced solar cells for front and rear side depositions[J]. *Journal of Applied Physics*, 2011, **109**(7): 073105.

[8] PEDRUEZA E, VALDES J L, CHIRVONY V, *et al*. Novel method of preparation of gold-nanoparticle-doped TiO_2 and SiO_2 plasmonic thin films: optical characterization and comparison with Maxwell - Garnett modeling[J]. *Advanced Functional Materials*, 2011, **21**(18): 3502-3507.

[9] GANGULY A, MONDAL A, DHAR J C, et al. Enhanced visible light absorption by TiO_2 film patterned with Ag nanoparticles arrays[J]. *Physica E: Low-dimensional Systems and Nanostructures*, 2013, **54**(12): 326-330.

[10] BECK F J, POLMAN A, CATCHPOLE K R. Tunable light trapping for solar cells using localized surface plasmons[J]. *Journal of Applied Physics*, 2009, **105**(11): 114310.

[11] XU Rui, WANG Xiao-dong, SONG Liang, *et al*. Influence of the light trapping induced by surface plasmons and antireflection film in crystalline silicon solar cells[J]. *Optics express*, 2012, **20**(5): 5061-5068.

[12] XU Yong-jun, CAI Qi-wen, YANG Xiao-xi, *et al*. Preparation of novel SiO_2 protected Ag thin films with high reflectivity by magnetron sputtering for solar front reflectors [J]. *Solar Energy Materials and Solar Cells*, 2012, **107**(2): 316-321.

[13] CHOY W C H, SHA W E I, LI Xuan-hua, *et al*. Multi-physical properties of plasmonic organic solar cells[J]. *Progress in Electromagnetics Research*, 2014, **146**(1): 25-46.

[14] HEDAYATI M K, FAUPEL F, ELBAHRI M. Review of plasmonic nanocomposite metamaterial absorber [J]. *Materials*, 2014, **7**(2): 1221-1248.

[15] HEDAYATI M K, JAVAHERIRAHIM M, MOZOONI B, *et al*. Design of a perfect black absorber at visible frequencies using plasmonic metamaterials[J]. *Advanced Materials*, 2011, **23**(45): 5410-5414.

[16] XU Rui, WANG Xiao-dong, LIU Wen, *et al*. Optimization of the dielectric layer thickness for surface-plasmon-induced light absorption for silicon solar cells[J]. *Japanese Journal of Applied Physics*, 2012, **51**(4R): 483-490.

[17] XIANG Yong, LI Teng, SUO Zhi-gang, *et al*. High ductility of a metal film adherent on a polymer substrate[J]. *Applied Physics Letters*, 2005, **87**(16): 161910.

[18] TRICE J, THOMAS D, FAVAZZA C, *et al*. Pulsed-laser-induced dewetting in nanoscopic metal films: Theory and experiments[J]. *Physical Review B*, 2007, **75**(23): 235439.

[19] VIANA C E, SILVA A N R D, MORIMOTO N I, *et al*. Analysis of SiO_2 thin films deposited by PECVD using an oxygen-TEOS-argon mixture [J]. *Brazilian Journal of Physics*, 2001, **31**(2): 299-303.

[20] BAI Yi-ming, WANG Jun, CHEN Nuo-fu, *et al*. Condensed matter: electronic structure, electrical, magnetic, and optical properties: dipolar and quadrupolar modes of SiO_2/Au nanoshell enhanced light trapping in thin film solar cells[J]. *Chinese Physics Letters*, 2011, **28**(8): 087306.

[21] ZHANG Shu-guang, ZHANG Xing-wang, YIN Zhi-gang, *et al*. Optimization of electroluminescence from n-ZnO/AlN/p-GaN light-emitting diodes by tailoring Ag localized surface plasmon[J]. *Journal of Applied Physics*, 2012, **112**(1): 013112.

[22] GAO Hong-li, ZHANG Xing-wang, YIN Zhi-gang, *et al*. Plasmon enhanced polymer solar cells by spin-coating Au nanoparticles on indium-tin-oxide substrate [J]. *Applied Physics Letters*, 2012, **101**(13): 133903.

[23] BAI Yi-ming, GAO Zheng, CHEN Nuo-fu, *et al*. Elimination of small-sized Ag nanoparticles via rapid thermal annealing for high efficiency light trapping structure [J]. *Applied Surface Science*, 2014, **315**(10): 1-7.

[24] BAI Yi-ming, WANG Jun, CHEN Nuo-fu, *et al*. Quantifying the effectiveness of SiO_2/ Au light trapping nanoshells for thin film poly-Si solar cells[J]. *Science China Technological Sciences*, 2010, **53**(8):2228-2231.

[25] BOHREN C F, HUFFMAN D R. Absorption and scattering of light by small particles[M]. New York, John Wiley & Sons, 2008.